J|A|C|S
ARTICLES
Published on Web 01/13/2004

Microwave Spectra and Structures of KrAuF, KrAgF, and KrAgBr; ^{83}Kr Nuclear Quadrupole Coupling and the Nature of Noble Gas−Noble Metal Halide Bonding

Jason M. Thomas, Nicholas R. Walker,† Stephen A. Cooke, and Michael C. L. Gerry*

Contribution from the Department of Chemistry, The University of British Columbia, 2036 Main Mall, Vancouver, B.C. Canada V6T 1Z1

Received July 16, 2003; E-mail: mgerry@chem.ubc.ca

Abstract: Microwave spectra of the complexes KrAuF and KrAgBr have been measured for the first time using a cavity pulsed jet Fourier transform microwave spectrometer. The samples were prepared by laser ablation of the metal from its solid and allowing the resulting plasma to react with an appropriate precursor (Kr, plus SF_6 or Br_2) contained in the backing gas of the jet (usually Ar). Rotational constants; geometries; centrifugal distortion constants; vibration frequencies; and ^{197}Au, ^{79}Br, and ^{81}Br nuclear quadrupole coupling constants have all been evaluated. The complexes are unusually rigid and have short Kr−Au and Kr−Ag bonds. The ^{197}Au nuclear quadrupole coupling constant differs radically from its value in an AuF monomer. In addition ^{83}Kr hyperfine structure has been measured for KrAuF and the previously reported complex KrAgF. The geometry of the latter has been reevaluated. Large values for the ^{83}Kr nuclear quadrupole coupling constants have been found for both complexes. Both the ^{197}Au and ^{83}Kr hyperfine constants indicate a large reorganization of the electron distribution on complex formation. A thorough assessment of the nature of the noble gas−noble metal bonding in these and related complexes (NgMX; Ng is a noble gas, M is a noble metal, and X is a halogen) has been carried out. The bond lengths are compared with sums of standard atomic and ionic radii. Ab initio calculations have produced dissociation energies along with Mulliken populations and other data on the electron distributions in the complexes. The origins of the rigidity, dissociation energies, and nuclear quadrupole coupling constants are considered. It is concluded that there is strong evidence for weak noble gas−noble metal chemical bonding in the complexes.

Introduction

Over the past few years, we have reported the microwave spectra of a series of linear complexes of the general formula NgMX, where Ng is a noble gas (particularly Ar or Kr), M is a noble metal (Cu, Ag, Au), and X is a halogen (F, Cl, Br); an example is ArAuCl.[1−5] The complexes and their spectra show unusual features not usually found for van der Waals complexes. The Ng−M bonds are short and range from ∼2.3 Å for Ar−Cu[1b] to ∼2.5 Å for Ar−Au[2,3] to ∼2.6 Å for Ar−Ag[1a] and ∼2.7 Å for Kr−Ag.[4,5] The molecules and, in particular, the Ng−M bonds, are rigid: the centrifugal distortion constants, which give a measure of molecular flexibility, and which are easily determined from the microwave spectra, are very small. The distortion constants also yielded estimates of the Ng−M stretching frequencies, all of which are above 100 cm^{-1}. The nuclear quadrupole coupling constants (NQCCs) of Cu and Au in the NgMX complexes are very different from those of the corresponding CuX and AuX monomers, consistent with a large rearrangement of the electron distribution near the metal nucleus on attachment of the Ng atom. The changes are ∼30−40% of those when X^- attaches to MX to form XMX^- ions (which are isoelectronic with NgMX).[1b,2,6] Interestingly the Cl and Br coupling constants undergo comparable fractional changes, but because the changes in their absolute values are rather less, they do not seem so dramatic.[1b,2]

The experimental results have been supported by ab initio, particularly MP2, calculations. Both the bond lengths and vibration frequencies are reproduced. Dissociation energies of several tens of kJ mol^{-1} have been estimated; these are considerably greater than values normally expected for neutral van der Waals complexes. (For example, the analogous complex Ar−NaCl has an estimated dissociation energy ∼8 kJ mol^{-1}.)[7] Mulliken populations suggest that there is a donation of ∼0.05−0.2 electron from Ng to MX. As well, MOLDEN plots indicate some *occupied* valence molecular orbitals which are significantly delocalized over the whole complex. Although the complexes

† Present address: Department of Chemistry, University of Bristol, Bristol BS8 1TS, U.K..

(1) (a) Evans, C. J.; Gerry, M. C. L. *J. Chem. Phys.* **2000**, *112*, 1321. (b) *J. Chem. Phys.* **2000**, *112*, 9363.
(2) Evans, C. J.; Lesarri, A.; Gerry, M. C. L. *J. Am. Chem. Soc.* **2000**, *122*, 6100.
(3) Evans, C. J.; Rubinoff, D. J.; Gerry, M. C. L. *Phys. Chem. Chem. Phys.* **2000**, *2*, 3943.
(4) Reynard, L. M.; Evans, C. J.; Gerry, M. C. L. *J. Mol. Spectrosc.* **2001**, *206*, 33.
(5) Walker, N. R.; Reynard, L. M.; Gerry, M. C. L. *J. Mol. Struct.* **2002**, *612*, 109.
(6) Viegers, T. P. A.; Trooster, J. M.; Bouten, P.; Rït, T. P. *J. Chem. Soc., Dalton Trans.* **1977**, 2074.
(7) Mizoguchi, A.; Endo, Y.; Ohshima, Y. *J. Chem. Phys.* **1998**, *109*, 10539.

might be considered largely as van der Waals complexes, there is thus evidence for weak noble gas−noble metal chemical bonding.

The observations are paralleled by some unusual properties of the $NgAu^+$ ions. Recently Bellert and Breckenridge[8] reviewed the properties of a wide range of NgM^+ complexes and found that they could almost all be accounted for with a simple electrostatic model. This was not the case for $NgAu^+$ (Ng = Ar, Kr, and especially Xe), which are rather more strongly bound than the model would suggest. The $XeCu^+$ and $XeAg^+$ complexes are apparently "normal". Although their deductions are based on results of earlier ab initio calculations,[9] the authors conclude that there is a real possibility that the Ng atom is showing partial σ-donor Lewis base character and plead for reliable experimental information on $XeAu^+$.

Shortly after the first reports of NgMX compounds were published, a report of the preparation and isolation in the solid state of $(AuXe_4^{2+})(Sb_2F_{11}^-)_2$ appeared.[10] In an atmosphere of Xe, this compound has been found to be stable enough for a structural determination by X-ray diffraction. The $AuXe_4^{2+}$ ion is square planar, with Au−Xe bond lengths of ∼2.74 Å, slightly greater than those of the Kr−Au and Ar−Au bonds in NgAuX. A strong Raman band at 129 cm^{-1} was found. Ab initio calculations gave Mulliken populations in this case which indicated donation of ∼0.4 electron from each Xe to Au and average Au−Xe bond energies of ∼200 kJ mol^{-1}. The trends are clearly consistent with those of the NgMX molecules, even though $AuXe_4^{2+}$ contains Au(II), while NgMX have M(I). Since then, it has been found mass spectrometrically that many MNg_4^{2+} ions are relatively stable,[11] suggesting that $AuXe_4^{2+}$ is merely the most stable of a long series of such ions.

Several other complexes containing Au−Xe bonds have been isolated.[12] Most of these contain Au(II), though one contains Au(III). In all cases, Au is four-coordinate in a square planar environment. The authors also report that they have been unable to detect complexes of Au(I). They furthermore predict that the prospect of synthesis of complexes containing Kr is poor. A complex containing an interaction between Cu^{2+} and Xe has recently been described[13] but is apparently the only example of a molecule in which Xe has been attached to Cu^{2+} in a solid-state environment. It is thus clear that our microwave spectroscopic experiments, which have revealed bonds of both Ar and Kr to Au(I), have provided an experimental technique, plus a wealth of structural information, unavailable to more traditional synthetic chemists.

Although our microwave spectroscopic studies of NgMX have in general been successful, there are still some open questions. For example, the Ar-containing complexes have been relatively easy to prepare, and the spectra of molecules with all permutations of M = Cu, Ag, Au and X = F, Cl, Br have been published.[1−3] Hitherto spectra of complexes containing Kr have been much more elusive, because optimum experimental conditions for their efficient preparation have been difficult to find. Spectra of only KrAuCl, KrAgCl, and KrAgF have been reported.[2,4,5]

Although it has been clear from the Cu and Au nuclear quadrupole coupling constants that there is a drastic rearrangement of the metal electron distribution on complex formation, there has hitherto been no comparable information for the noble gas. Such information has been unavailable for Ar because it has no quadrupolar nucleus. However, krypton has an isotope, ^{83}Kr, with $I = {}^9/_2$; unfortunately it is only 11.5% abundant, so if the spectrum of a complex is weak overall, the prospect of seeing ^{83}Kr hyperfine structure is slim.

Recent changes in our sample preparation technique have significantly improved the signal-to-noise ratios of the spectra of the KrMX complexes. It has now been possible to observe spectra of new KrMX complexes and of missing isotopomers of old ones. Accordingly, the present paper reports the microwave spectra of two new Kr complexes, KrAuF and KrAgBr. In addition, spectra have been found for the first time for two ^{83}Kr-containing molecules, namely KrAgF and KrAuF. Large ^{83}Kr nuclear quadrupole coupling has given the first direct measure of the redistribution of the noble gas electron density on complex formation. As a result of this discovery, the nature of the noble gas−noble metal bonding has been comprehensively reassessed.

Experimental Methods

The spectra were measured with a cavity pulsed jet Fourier transform microwave (FTMW) spectrometer of the Balle−Flygare type;[14] it has been described in detail earlier.[15] It contains a Fabry−Perot cavity cell consisting of two spherical mirrors 28.5 cm in diameter, of radius of curvature 38 cm, held approximately 30 cm apart. One mirror is held fixed, while the other can be moved to tune the cavity. The samples were studied entrained in pulsed supersonic jets of noble gas, which were injected into the cavity from a nozzle (General Valve, Series 9) mounted near the center of the fixed mirror. Although this arrangement optimizes both the sensitivity and resolution of the spectrometer, it also causes each line to be split to a doublet by the Doppler effect.

The complexes were produced using the laser ablation source which has been described in detail earlier.[16] A metal sample was held in front of the nozzle and ablated with the second harmonic (532 nm, 5−10 mJ/pulse) of an Nd:YAG laser. The metal target usually consisted of a 5 mm diameter rod; it was continuously rotated and translated to expose a fresh surface for each laser shot. In some circumstances, notably in the initial search for lines of KrAgBr, and in the studies of $^{83}KrAgF$, the rod was replaced by a piece of ^{107}Ag foil (99.9% isotopically abundant), wrapped round a 5 mm diameter glass rod: since Ag has two isotopes of natural abundance ∼50%, this was used chiefly to increase the signal-to-noise ratio for molecules containing this isotope. For the fluorides, the precursor gas consisted of 0.1% SF_6 contained in pure Kr (for KrAuF) or 20% Kr in Ar (for KrAgF). For KrAgBr, 0.1% Br_2 was contained in a mixture of 7% Kr in Ar. The backing gas pressures were 5−7 atm.

The properties of the expansion change with backing gas composition, as indicated by a change in Doppler splitting, which is a function of the molecular velocity in the jet. Accordingly, the laser delay had to be adjusted to give an optimum signal-to-noise ratio for each backing gas or gas mixture. The most intense spectra, in all cases, were obtained using a microwave pulse width of 0.2 μs, the shortest available for the spectrometer, consistent with a high dipole moment for the complexes.

(8) Bellert, D.; Breckenridge, W. H. *Chem. Rev.* **2002**, *102*, 1595.
(9) Schröder, D.; Schwarz, H.; Hrusak, J.; Pyykkö, P. *Inorg. Chem.* **1998**, *37*, 624.
(10) Seidel, S.; Seppelt, K. *Science* **2000**, *290*, 117.
(11) Walker, N. R.; Wright, R. R.; Barran, P. E.; Cox, H.; Stace, A. J. *J. Chem. Phys.* **2001**, *114*, 5562.
(12) Drews, T.; Seidel, S.; Seppelt, K. *Angew. Chem., Int. Ed.* **2002**, *41*, 454.
(13) Qiu, X.; Nazin, G. V.; Hotzel, A.; Ho, W. *J. Am. Chem. Soc.* **2002**, *124*, 14804.
(14) Balle, T. J.; Flygare, W. H. *Rev. Sci. Instrum.* **1981**, *52* 33.
(15) Xu, Y.; Jäger, W.; Gerry, M. C. L. *J. Mol. Spectrosc.* **1992**, *151*, 206.
(16) Walker, K. A.; Gerry, M. C. L. *J. Mol. Spectrosc.* **1997**, *182*, 178.

Though the strongest lines of KrAuF could be seen with fewer than 300 pulses, the lines of ^{83}Kr isotopomers often required a few thousand pulses to produce a clear signal. For KrAgBr, 2000−3000 pulses were needed for a good signal-to-noise ratio.

The frequency range of the present experiments was 6−18 GHz. Line frequency measurements were referenced to a Loran frequency standard accurate to 1 part in 10^{10}. Observed line widths were ∼7−10 kHz fwhm; the measured line frequencies are estimated to be accurate to ±1 kHz.

Quantum Chemical Calculations

Quantum chemical calculations were carried out at the second-order Møller−Plesset (MP2)[17] level of theory, using the GAUSSIAN 98 suite of programs.[18] For Au and Ag, relativistic effective core potentials (RECP) were used. The basis set for Au was a (9s/7p/6d/3f) Gaussian basis set contracted to (8s/4p/5d/3f).[19,20] The RECP for Ag left 19 valence electrons ($4s^24p^64d^{10}5s^1$). The RECP for Ag and the optimized (31111s/22111p/411d) Gaussian basis sets were taken from Andrae et al.[21] The Ag basis set was further augmented with two f-functions ($\alpha_f = 3.1235$ and $\alpha_f = 1.3375$),[22] because it has been shown that at least one f-symmetry function is needed to produce reliable correlation energies for the Ag 4d shell.[23] For F, Br, and Kr, we used the simple 6-311G** basis set, the aug-cc-pVTZ basis set,[24] and the cc-pVTZ basis set,[24] respectively. The counterpoise correction was applied to account for basis set superposition error (BSSE).[25] All structures were constrained to a linear geometry.

Experimental Results and Analysis

KrAuF. Initial prediction of the rotational constants of KrAuF was carried out using trends found for previously observed Ar- and Kr-containing complexes of Au and Ag halides. The first lines were found near 10 479 MHz and assigned to the $J = 5-4$ transition of ^{84}KrAuF. The observed pattern was a doublet of doublets, which was attributed to ^{197}Au nuclear quadrupole coupling; as was anticipated, this gave an ^{197}Au nuclear quadrupole coupling constant somewhat bigger in magnitude than that of ArAuF[3] and suggested strongly that lines of KrAuF had been found. The signal disappeared when laser ablation was omitted. Further confirmation was obtained by locating transitions for other *J*-values and for the ^{82}Kr- and ^{86}Kr-containing isotopomers. The spectra of each of these isotopomers were moderately strong; an example transition is depicted in Figure 1.

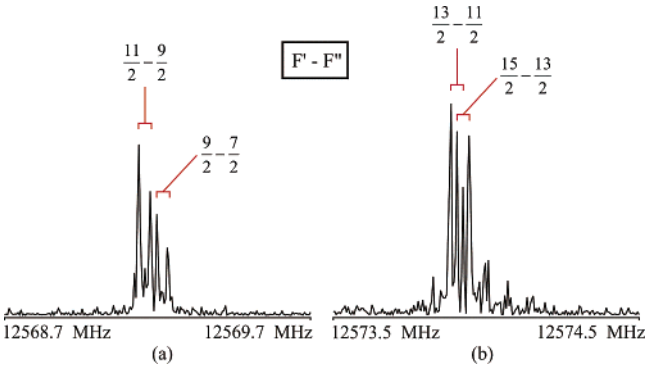

Figure 1. Observed lines of the $J = 6-5$ transitions of ^{84}Kr^{197}Au^{19}F. Experimental conditions: 0.2 μs microwave pulse width; ∼0.1% SF_6 in Kr at 5−7 atm backing pressure; 600(a)−300(b) averaging cycles; 4k transform (no zero filling).

Table 1. Spectroscopic Constants of KrAuF

isotopomer	B_0 (MHz)	D_J (kHz)	*eQq* (^{83}Kr) (MHz)	*eQq* (^{197}Au) (MHz)
^{82}KrAuF	1063.615 560(62)[a]	0.165 55(68)		−404.749(26)
^{83}KrAuF	1055.561 007(86)	0.1681(11)	189.965(46)	−404.573(38)
^{84}KrAuF	1047.704 999(57)	0.162 56(58)		−404.775(26)
^{86}KrAuF	1032.456 775(59)	0.159 43(62)		−404.781(26)

[a] Numbers in parentheses are one standard deviation in units of the last significant figure.

The measured frequencies are given with their assignments in the Supporting Information; the coupling scheme $\mathbf{J} + \mathbf{I_{Au}} = \mathbf{F}$ is used. The spectra were analyzed using Pickett's global least-squares fitting program SPFIT,[26] with each isotopomer treated separately. The resulting spectroscopic constants are in Table 1, along with those of ^{83}KrAuF, whose spectrum is discussed separately below.

KrAgBr. As with KrAuF, the rotational constants of KrAgBr were initially predicted using trends in bond lengths in other NgMX molecules. Initial searches were carried out using the isotopically pure ^{107}Ag foil, to increase signal strengths and to ease the assignment of lines to isotopomers containing ^{107}Ag. Weak signals were detected within 15 MHz of the frequency predicted for ^{84}Kr^{107}Ag^{79}Br; they showed a quadrupole splitting pattern similar to that found for ArAgBr. Similar groups of lines were found for several further rotational transitions separated by $\sim 2B_o$, consistent with a linear molecule. The signals disappeared when laser ablation was omitted, confirming that they were due to KrAgBr.

Although both ^{79}Br and ^{81}Br are quadrupolar nuclei with $I = {}^3/_2$, they have different quadrupole moments and thus different quadrupole coupling constants. From a comparison of the Br coupling constant with those of ArAgBr,[1a] the groups of lines initially found were actually assigned to ^{84}Kr^{107}Ag^{81}Br. From its rotational constant, and assuming the AgBr distance to be unchanged from the monomer,[27] the KrAg bond length was estimated. These bond lengths were then used to predict the rotational constant and frequencies of ^{84}Kr^{107}Ag^{79}Br. Lines due to this isotopomer were found within a few MHz of the prediction. The assignment was confirmed by comparison of the ^{79}Br and ^{81}Br quadrupole coupling constants.

The spectra of four other isotopomers of KrAgBr were predicted and measured in a similar way. Transitions of

(17) Møller, C. S.; Plesset, M. S. *Phys. Rev.* **1934**, *46*, 618.
(18) Frisch, M. J.; Truchs, G. W.; Schlegel, H. B.; Scuseria, G. E.; Robb, M. A.; Cheeseman, J. R.; Zakrzewski, V. G.; Montgomery, J. A., Jr.; Stratmann, R. E.; Burant, J. C.; Dapprich, S.; Millam, J. M.; Daniels, A. D.; Kudin, K. N.; Strain, M. C.; Farkas, O.; Tomasi, J.; Barone, V.; Cossi, M.; Cammi, R.; Mennucci, B.; Pomelli, C.; Adams, C.; Clifford, S.; Ochterski, J.; Peterssohn, G. A.; Ayala, P. Y.; Cui, Q.; Morokuma, K.; Malick, D. K.; Rabuck, A. D.; Ragavachari, J. B.; Forsman, J. B.; Ciolowski, J.; Ortiz, J. V.; Baboul, A. G.; Stefanov, B. B.; Liu, G.; Liahsenko, A.; Piskorz, P.; Komaromi, I.; Gemperts, R.; Martin, R. L.; Fox, D. J.; Keith, T.; Al-Laham, M. A.; Peng, C. Y.; Nannayakkara, A.; Gonzalez, C.; Challacombe, M.; Gill, P. M. W.; Johnson, B.; Chen, W.; Wong, M. W.; Andres, J. L.; Head-Gordon, M.; Replogle, E. S.; Pople, J. A. *GAUSSIAN 98*, revision A.7; Gaussian, Inc.: Pittsburgh, PA, 1998.
(19) Schwerdtfeger, P. *Chem. Phys. Lett.* **1991**, *183*, 457.
(20) Schwerdtfeger, P.; Dolg, M.; Schwarz, W. H. E.; Bowmaker, G. A.; Boyd, P. D. W. *J. Chem. Phys.* **1989**, *91*, 1762.
(21) Andrae, D.; Häusermann, V.; Dolg, M.; Stoll, H.; Preus, H. *Theor. Chim. Acta* **1990**, *27*, 213.
(22) Antes, I.; Dapprich, S.; Frenking, G.; Schwerdtfeger, P. *Inorg. Chem.* **1996**, *35*, 2089.
(23) Ramirez-Solis, A.; Daudey, J. P.; Ruiz, M. E.; Novaro, O. *Z. Phys. D: At., Mol. Clusters* **1990**, *15*, 71.
(24) (a)Woon, D. E.; Dunning, T. H., Jr. *J. Chem. Phys.* **1993**, *98*, 1358. (b) Wilson, A. K.; Woon, D. E.; Peterson, K. A.; Dunning, T. H., Jr. *J. Chem. Phys.* **1999**, *110*, 7667.
(25) Hobza, P.; Zahraduik, R. *Chem. Rev.* **1988**, *88*, 871.
(26) Pickett, H. M. *J. Mol. Spectrosc.* **1991**, *148*, 371.
(27) Hoeft, J.; Lovas, F. J.; Tiemann, E.; Törring, T. *Z. Naturforsch.* **1970**, *25a*, 35.

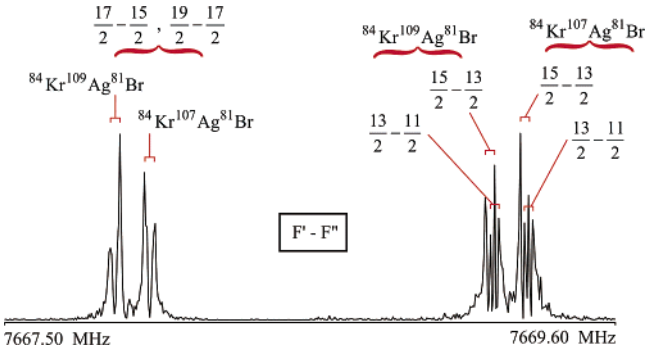

Figure 2. $J = 8-7$ transitions of $^{84}Kr^{107}Ag^{81}Br$ and $^{84}Kr^{109}Ag^{81}Br$, showing ^{81}Br hyperfine structure. The two patterns are nearly overlapped because Ag is near the center of mass of the molecule. Experimental conditions: 0.2 μs microwave pulse width; ~0.1% Br_2 and ~7% Kr in Ar at 5−7 atm backing pressure; 3000 averaging cycles; 4k transform (no zero filling).

Table 2. Spectroscopic Constants of KrAgBr

isotopomer	B_0 (MHz)	D_J (kHz)	eQq (Br) (MHz)
$^{84}Kr^{107}Ag^{79}Br$	485.065 579(41)[a]	0.044 73(17)	271.91(12)
$^{84}Kr^{109}Ag^{79}Br$	485.053 446(56)	0.044 33(21)	271.90(16)
$^{84}Kr^{107}Ag^{81}Br$	479.288 739(45)	0.043 30(19)	226.99(12)
$^{84}Kr^{109}Ag^{81}Br$	479.280 936(45)	0.043 02(19)	226.82(12)
$^{86}Kr^{107}Ag^{81}Br$	473.482 450(73)	0.040 04(32)	226.16(18)
$^{86}Kr^{109}Ag^{81}Br$	473.471 585(73)	0.042 55(32)	226.96(18)

[a] Numbers in parentheses are standard deviations in units of the last significant figure.

molecules containing ^{109}Ag were observed using the Ag rod containing the isotopes in their natural abundances. The spectra were much weaker than those of KrAuF and required 10 times as many pulses for a comparable signal-to-noise ratio. An example transition is in Figure 2. Overall seven $(J + 1) - J$ transitions were observed for the ^{84}Kr-containing isotopomers, and five, for the ^{86}Kr-containing isotopomers. Four quadrupole splitting components were measurable for most observed transitions.

The measured transition frequencies for all observed isotopomers of KrAgBr are in the Supporting Information. The coupling scheme $\mathbf{J} + \mathbf{I_{Br}} = \mathbf{F}$ is used. Again, the spectra were analyzed with Pickett's program SPFIT,[26] with each isotopomer treated separately. The resulting spectroscopic constants are in Table 2.

^{83}Kr Hyperfine Structure. A major objective of this study was to measure the ^{83}Kr NQCCs in KrMX compounds, since these would provide a direct probe of the nature of the bonding between Kr and the metal M. The spectra were expected to be weak because ^{83}Kr has only 11.5% abundance; also, its nuclear spin $I = {}^9/_2$, which in turn would cause each rotational transition to split to ~10 hyperfine components with consequent further loss of line intensity.

The ideal compound for an initial search was $^{83}Kr^{107}Ag^{19}F$. Since both ^{107}Ag and ^{19}F have $I = {}^1/_2$, they have no nuclear electric quadrupole moment, so that all hyperfine splittings would be due to ^{83}Kr alone. Also, both ^{19}F and ^{107}Ag were ~100% abundant in the experiment (^{19}F naturally, and ^{107}Ag by enrichment), so the relative abundance would be that of ^{83}Kr itself. It was straightforward to calculate the rotational constant, and hence the basic rotational transition frequencies, from the previously obtained geometry.[5] The only significant unknown was the desired ^{83}Kr NQCC, but a generic pattern could be predicted.

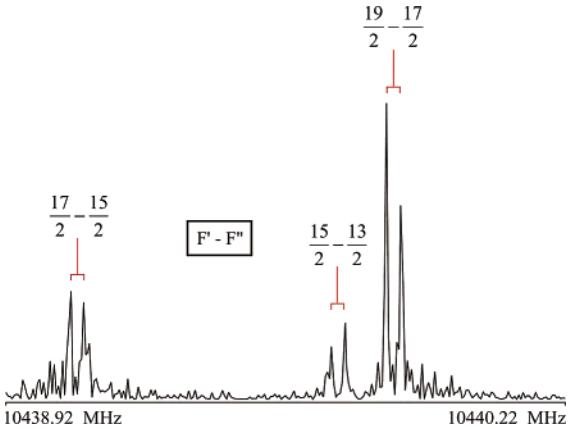

Figure 3. A portion of the hyperfine structure of the $J = 5-4$ transition of $^{83}Kr^{107}Ag^{19}F$. Experimental conditions: 0.2 μs microwave pulse width; ~0.1% SF_6, 20% Kr in Ar at 5−7 atm backing pressure; 5700 averaging cycles; 4k transform (no zero filling).

Table 3. Spectroscopic Constants of KrAgF

isotopomer	B_0 (MHz)	D_J (kHz)	eQq (^{83}Kr) (MHz)	reference
$^{83}Kr^{107}Ag^{19}F$	1044.050 32(63)[a]	0.31551(90)	105.401(16)	this work
$^{84}Kr^{107}Ag^{19}F$	1037.548 34(13)	0.3116(13)		5
$^{84}Kr^{109}Ag^{19}F$	1034.425 53(13)	0.3125(13)		5
$^{86}Kr^{107}Ag^{19}F$	1024.930 70(10)	0.3057(11)		5
$^{86}Kr^{109}Ag^{19}F$	1021.765 97(13)	0.3059(13)		5

[a] Numbers in parentheses are one standard deviation in units of the last significant figure.

After some initial searching, some weak transitions were found which could be assigned to this isotopomer. Altogether lines of five $(J + 1) - J$ rotational transitions were assigned and measured. Their frequencies and quantum number assignments in the coupling scheme $\mathbf{J} + \mathbf{I_{Kr}} = \mathbf{F}$ are given in the Supporting Information. A portion of the observed hyperfine structure of the $J = 5-4$ transition is depicted in Figure 3. The spectroscopic constants, again derived using SPFIT,[26] are in Table 3. For comparison purposes, this table also contains the constants reported earlier for the other isotopomers.[5]

The situation was less favorable for $^{83}Kr^{197}Au^{19}F$. Although ^{197}Au and ^{19}F both have 100% natural abundance, ^{197}Au also has a quadrupolar nucleus ($I = {}^3/_2$), which further divided the transition intensities. Prediction of the rotational constant was again straightforward, both by interpolation between those of the other isotopomers and by using the geometry derived from them. Prediction of the hyperfine patterns was awkward. Although eQq (^{197}Au) was known from other isotopomers, that of ^{83}Kr had to be guessed.

Given that it was likely that the bonding between Kr and Au would be stronger than that between Kr and Ag and, hence, that the electron distribution at Kr would be less spherical in KrAuF, a series of patterns was predicted with eQq (^{83}Kr) starting at its value in ^{83}KrAgF and increasing in magnitude. Ultimately a close enough match between predicted and observed patterns was found that an assignment could be made. The observed lines were exceedingly weak; an example, part of the $J = 6-5$ transition, is given in Figure 4.

In total, lines of three $(J + 1) - J$ transitions were assigned and measured for $^{83}Kr^{197}Au^{19}F$. Their frequencies and quantum number assignments are in the Supporting Information. The coupling scheme used is $\mathbf{J} + \mathbf{I_{Au}} = \mathbf{F_1}$; $\mathbf{F_1} + \mathbf{I_{Kr}} = \mathbf{F}$. The

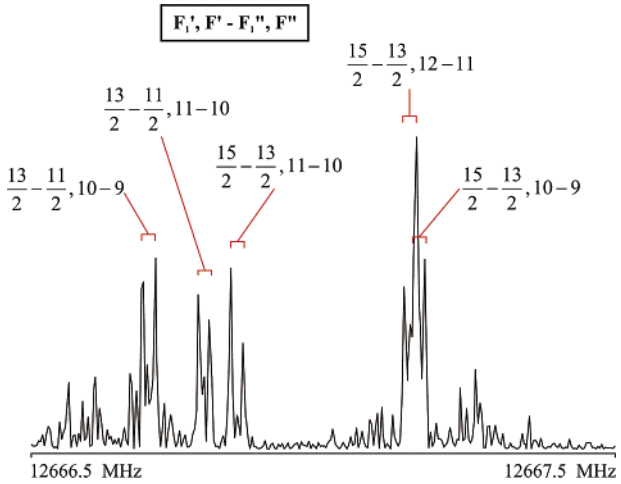

Figure 4. Portion of the hyperfine structure of $J = 6-5$ transition of $^{83}Kr^{197}Au^{19}F$. Experimental conditions: 0.2 μs microwave pulse width; ~0.1% SF_6 in Kr at 5−7 atm backing pressure; 7000 averaging cycles; 4k transform (no zero filling).

Table 4. Geometry[a] of KrAuF

method	r(Kr–Au)	r(Au–F)	comments
r_o	2.463 253(15)[b]	1.918[c]	
$r_{I\epsilon}$	2.461 222(11)	1.918[c]	$\epsilon = 0.645(3)$ uÅ^2
$r_m^{(1)}$	2.459 669(21)	1.918[c]	$c = 0.0519(3)$ u$^{1/2}$Å
MP2	2.452	1.952	
MP2[d]	2.454	1.913	

[a] Bond distances in Å. [b] Numbers in parentheses are one standard deviation in units of the last significant figure. [c] Au−F bond distance fixed at r_e of AuF.[31] [d] Values predicted in ref 32.

Table 5. Geometry[a] of KrAgBr

method	r(Kr–Ag)	r(Ag–Br)	comments
r_o	2.6681(39)[b]	2.3851(42)	
$r_{I\epsilon}$	2.6652(13)	2.3851(13)	$\epsilon = 1.52(25)$ uÅ^2
$r_m^{(1)}$	2.6633(15)	2.3834(15)	$c = 0.094(15)$ u$^{1/2}$Å
$r_m^{(2)}$	2.66216(17)	2.382 25(15)	$c = 0.2193(75)$ u$^{1/2}$Å; $d = -0.434(25)$ u$^{1/2}$Å^2
MP2	2.689	2.397	
r_e(AgBr)[c]		2.393 100(3)	

[a] Bond distances in Å. [b] Numbers in parentheses are one standard deviation in units of the last significant figure. [c] Reference 33.

spectroscopic constants derived using SPFIT[26] are in Table 1 in comparison with those of the other isotopomers.

Structures of the Complexes

Molecular Geometries. The experimental rotational constants have been used to evaluate geometries for all the complexes studied. For KrAuF and KrAgBr, these are the first geometries determined. That of KrAgF is an update of the one in ref 5, with the addition of the results newly obtained here. Although the rotational constants for several isotopic species have been evaluated, they are all for the ground vibrational state, and equilibrium (r_e) geometries are not available. Instead it has been necessary to make approximations.

The first approximation is a ground-state effective (r_o) geometry. In this case, the ground-state moments of inertia I_o are assumed to be given by rigid rotor formulas with no dependence of the structure on isotopomer or vibrations:

$$I_o = I_{rigid}(r_o) \qquad (1)$$

The r_o geometry is obtained by a least-squares fit of the I_o values to the bond lengths.

Since the ground-state rotational constants (B_o) and moments of inertia (I_o) do indeed have a vibrational dependence, this can be accounted for, at least partially, with an extra parameter, designated ϵ, in the least-squares fit. If ϵ is assumed to be independent of isotopomer, then I_o is given by

$$I_o = I_{rigid}(r_{I\epsilon}) + \epsilon \qquad (2)$$

Thus, in the second fitting method, the bond lengths plus ϵ are fit to the experimental I_o values. This gives the so-called $r_{I\epsilon}$ geometry.[28] When there is a large number of isotopic data, this is equivalent to the earlier substitution (r_s) geometry.[29]

To account for the isotopic mass dependence of ϵ, Watson et al.[30] derived the r_m geometries. These geometries are believed to provide the best approximations to equilibrium (r_e) geometries available from ground-state data alone. For a linear triatomic molecule, they are obtained using

$$I_o = I_m(r_m) + c(I_m)^{1/2} + d\left(\frac{m_1 m_2 m_3}{M}\right)^{1/4} \qquad (3)$$

where $I_m(r_m)$ is I_{rigid} using r_m bond lengths and c and d are constants; m_1, m_2, and m_3 are the atomic masses, and M is the molecular mass. In an $r_m^{(1)}$ fit, d is set to zero; in an $r_m^{(2)}$ fit, both c and d are included as fitting parameters.

For KrAuF, the very limited amount of data and, in particular, the fact that isotopic substitutions could be made only at Kr caused least-squares fits to both lengths to produce perfectly correlated values. It thus became necessary to fix one bond length; this was chosen to be r(AuF) which was held at its r_e value in the AuF monomer.[31] This permitted r_o, $r_{I\epsilon}$, and $r_m^{(1)}$ values for r(KrAu) to be determined; the results are in Table 4. Table 4 also contains the values from the MP2 calculation. As with ArAuF,[3] the calculated Ng−Au distance agrees well with those from the experimental data, while the MP2 AuF distance is bigger by ~0.03 Å. Although because of the assumption made the detailed comparison is suspect, the assumed experimental value and the ab initio value are in general agreement. It is interesting to note, in addition, that some recently published ab initio values,[32] also in Table 4, give a very similar Kr−Au distance, as well as an AuF distance which agrees better with the assumed experimental value.

For KrAgBr, for which spectra of six isotopic species were observed, and for which isotopic substitutions were made at all atoms, full least-squares fits were carried out to produce r_o, $r_{I\epsilon}$, $r_m^{(1)}$, and $r_m^{(2)}$ values. The results are in Table 5. Well-determined values have been obtained in each case. This is particularly so for the $r_m^{(2)}$ values, and probably results because the Ag atom is very near the center of mass of the complex.[30] The ab initio MP2 bond lengths are included in Table 5 for comparison, and show reasonable agreement with the experimental values. The Ag−Br bond length is very similar to that of the AgBr monomer, also given in Table 5.

The newly determined rotational constant of $^{83}Kr^{107}AgF$ was combined with those published earlier[5] to update the geometry

(28) Rudolph, H. D. *Struct. Chem.* **1991**, *2*, 581.
(29) Costain, C. C. *J. Chem. Phys.* **1958**, *29*, 864.
(30) Watson, J. K. G.; Roytburg, A.; Ulrich, W. *J. Mol. Spectrosc.* **1999**, *196*, 102.
(31) Evans, C. J.; Gerry, M. C. L. *J. Am. Chem. Soc.* **2000**, *122*, 1560.
(32) Lovallo, C. C.; Klobukowski, M. *Chem. Phys. Lett.* **2002**, *368*, 589.

Table 6. Geometry[a] of KrAgF

method	r(Kr–Ag)	r(Ag–F)	comments
r_o	2.600 98(5)[b]	1.9842(15)	
$r_{I\epsilon}$	2.601 64(13)	1.9760(10)	$\epsilon = 0.687(81)$ uÅ^2
$r_m^{(1)}$	2.599 81(18)	1.9747(12)	$c = 0.0622(75)$ u$^{1/2}$Å
$r_m^{(2)c}$	2.594 15	1.956 696	$c = 0.429$ u$^{1/2}$Å; $d = -0.859$ u$^{1/2}$Å^2
MP2	2.6009	1.9645	
MP2[d]	2.609	1.969	
r_e (AgF)[e]		1.983 17	

[a] Bond distances in Å. [b] Numbers in parentheses are one standard deviation in units of the last significant figure. [c] Results of exact calculation presented in ref 5. [d] Reference 32. [e] Reference 33.

of the complex. Again r_o, $r_{I\epsilon}$, $r_m^{(1)}$, and $r_m^{(2)}$ values were obtained. The first three were evaluated by least-squares fitting. Since the $r_m^{(2)}$ fit was indeterminate, probably because no isotopic substitution could be made at F, the values given are the result of an exact calculation given in ref 5. The results are in Table 6. The r_o values are apparently better determined than those given in ref 5, but the agreement is within the earlier standard deviations. On the other hand, the new $r_{I\epsilon}$ and $r_m^{(1)}$ values are less well-determined than the earlier values; the agreement this time is within the present standard deviations. In any case, the results agree well with the MP2 values, which are also in Table 6. The recently published ab initio values[32] show comparable agreement. It is notable that r(Ag−F) has a value very similar to that found in an uncomplexed AgF monomer (1.983 17 Å).[33]

The NgM bond lengths available to date are given in comparison with ab initio values in Table 7. For comparison purposes, this table also contains the bond lengths of several related species, as discussed below.

Vibration Frequencies and Dissociation Energies. The centrifugal distortion constants D_J of both the ArMX and KrMX complexes are very small, indicating that the complexes are remarkably rigid. The constants are over an order of magnitude smaller than that of Ar−NaCl, which shows all the characteristics usually expected of a van der Waals complex.[7] For a given MX, the distortion constant of KrMX is smaller than that of ArMX, chiefly, though not entirely, because of the greater mass of Kr. In particular, this applies to the ArAuF/KrAuF and ArAgBr/KrAgBr pairs. These data are all summarized in Table 7.

The Ng−M stretching frequencies, ω(NgM), have been estimated from the distortion constants D_J using the pseudodiatomic approximation:[34]

$$\omega(\mathrm{NgM}) = \left(\frac{4B_o}{D_J}^3\right)^{1/2} \qquad (4)$$

For KrAuF and KrAgBr, these are 176 and 106 cm^{-1}, respectively. The values for all complexes studied to date are also in Table 7. All are greater than 100 cm^{-1} (in many cases much greater) and considerably greater than those typically found for neutral van der Waals complexes (∼20 cm^{-1}). They are much closer to those of chemically bonded species. Table 7 also contains the corresponding values from the MP2 calculations; there is clearly excellent agreement. This agreement, plus the fact that the AuX frequencies (ω(AuX), also in Table 7) are considerably higher justifies the use of the pseudodiatomic approximation.

Parenthetically, the MX stretching frequencies ω(MX), all calculated ab initio for the complexes (Table 7), are each significantly greater than those of the corresponding MX monomer. This suggests in turn a significant redistribution of the MX electron density on complex formation.

To account for the mass dependence of the NgM stretching frequencies and, hence, obtain a better measure of the rigidity of the complexes, the Ng−M stretching force constants k(Ng−M) have been obtained, again using a pseudodiatomic approximation. These values are also in Table 7. For each noble gas−metal combination, there is a clear decrease in k going from the fluoride to the chloride to the bromide, which parallels increases in the NgM bond length. For a given MX monomer, the force constant k is always bigger for the KrM bond than for the ArM bond.

For most complexes, including KrAuF, KrAgF, and KrAgBr, the Ng−M dissociation energy D_e has been calculated ab initio. Two sets of calculations have been carried out. For the first set, which includes values reported in our earlier work,[1−5] basis set superposition error (BSSE) was ignored. In the second set, BSSE has been accounted for using the counterpoise correction.[25] The results of both sets of calculations are in Table 7. While in all cases accounting for BSSE reduces the predicted values of D_e, these changes are quite small for the ArMX complexes (∼10% in general). For the KrMX complexes, the reductions are nearer 40% and suggest that the D_e(Kr−M) values are only slightly larger than the D_e(Ar−M) values. However, the recent independent study,[32] using a different program and basis set, also corrected for BSSE, gave considerably larger D_e(Kr−M) values. The accuracy of the ab initio calculations is thus questionable. However, all the dissociation energies are relatively large and considerably bigger than those typical of most van der Waals bonds of neutral species (<10 kJ mol^{-1}). KrAuF has the highest value calculated thus far, 58−71 kJ mol^{-1}, which makes it bigger than the KrF bond energy in KrF_2 (50 kJ mol^{-1})[45] and about one-half the XeF bond energy in XeF_2 (133 kJ mol^{-1}).[46]

Table 7 also contains for comparison purposes results of ab initio calculations for complexes of the type $NgCuNg^+$[37] and $NgAuNg^+$.[43] These calculations did not account for BSSE. All these ions are valence isoelectronic with NgMX complexes. The predicted bond lengths, stretching frequencies, and NgM dissociation energies of $NgMNg^+$ and NgMX are all comparable.

(33) (a) Hoeft, J.; Lovas, F. J.; Tiemann, E.; Törring, T. *Z. Naturforsch.* **1970**, *25a*, 35; (b) *Z. Naturforsch.* **1971**, *26a*, 240.
(34) Kratzer, A. *Z. Phys.* **1920**, *3*, 289.
(35) Ahmed, F.; Barrow, R. F.; Chojmicki, A. H.; Dufour, C.; Schamps, J. *J. Phys. B* **1982**, *15*, 3001.
(36) (a) Manson, E. L.; DeLucia, F. C.; Gordy, W. *J. Chem. Phys.* **1975**, *62*, 1040. (b) *ibid* **1975**, *63*, 2724.
(37) Bauschlicher, C. W., Jr.; Partridge, H.; Langhoff, S. R. *Chem. Phys. Lett.* **1990**, *165*, 272.
(38) Barrow, R. F.; Clements, R. M. *Proc. R. Soc. London, Ser. A* **1971**, *322*, 243.
(39) (a) Brice, B. A. *Phys. Rev.* **1931**, *35*, 960. (b) Pearson, E. F.; Gordy, W. *Phys. Rev. B* **1966**, *152*, 42.
(40) Brice, B. A. *Phys. Rev.* **1931**, *38*, 658.
(41) Andreev, S.; Bel Bruno, J. J. *Chem. Phys. Lett.* **2000**, *329*, 490−494.
(42) Evans, C. J.; Gerry, M. C. L. *J. Mol. Spectrosc.* **2000**, *203*, 105.
(43) Pyykkö, P. *J. Am. Chem. Soc.* **1995**, *117*, 2067.
(44) Ohshima, Y.; Iida, M.: Endo, Y. *J. Chem. Phys.* **1990**, *92*, 3990.
(45) Lehmann, J. F.; Mercier, H. P. A.; Schrobilgen, G. J. *Coord. Chem. Rev.* **2002**, *233*−*234*, 1.
(46) Bartlett, N.; Sladky, F. O. In *Comprehensive Inorganic Chemistry*; Bailar, J. C., Emeléus, H. J., Nyholm, R., Trotman-Dickenson, A. F., Eds.; Pergamon: Oxford, 1973; pp 213−330.

Table 7. Ng−M Bond Lengths (r), Centrifugal Distortion Constants (D_J), Stretching Frequencies (ω), Force Constants (k), and Calculated Dissociation Energies (D_e) of Noble Gas−Noble Metal Halides and Related Complexes

complex	r(NgM)/Å e(a)[a]	D_J/kHz $\times 10^2$	ω(NgM)/cm^{-1} e(a)[b]	ω(MX)/cm^{-1} c(m)[c]	k(NgM) /Nm^{-1}[d]	D_e/kJ mol^{-1} c(u)[e]
ArCuF[f]	2.22(2.19)	94	224(228)	674(621[g])	79	44, 37[h](47)
ArCuCl[f]	2.27(2.24)	34	197(190)	456(418[i])	65	33, 28[h](37)
ArCuBr[f]	2.30(2.26)	12	170(164)	350(313[j])	53	
ArCuAr^{+}[k]	(2.34)					(41)
KrCuKr^{+}[k]	(2.42)					(58)
ArAgF[l]	2.56(2.56)	95	141(127)	541(513[m])	36	14, 18[h](17)
ArAgCl[l]	2.61(2.59)	35	135(120)	357(344[n])	34	16[h](14)
ArAgBr[l]	2.64	11	124	(251[o])	30	
KrAgF[p]	2.59(2.60)	31	125(113)	544(513[m])	48	17, 28[h](32)
KrAgCl[q]	2.64(2.63)	13	117(105)	352(344[n])	43	15, 26[h](28)
KrAgBr[r]	2.66(2.69)	4	106(89)	255(247[o])	38	17(25)
ArAuF[s]	2.39(2.39)	51	221(214)	583(544[t])	97	55, 50[h](59)
ArAuCl[u]	2.47(2.46)	21	198(184)	413(383[v])	78	42, 38[h](47)
ArAuBr[s]	2.50(2.49)	6	178(165)	286(264[v])	65	
ArAuAr^{+}[w]	(2.54)		(141, 201)[w]			(44)
KrAuF[r]	2.46(2.45)	16	176(184)	(544[t])	110	58, 71[h] (86)
KrAuCl[u]	2.52(2.51)	8	161(163)	409(383[v])	94	44, 56[h] (72)
KrAuKr^{+}[w]	(2.57)		(126, 186)[w]			(69)
ArNaCl[x]	2.89	900	21		0.6	(8)
ArHg[y]	4.05		22			

[a] e = results of experiment. a = values calculated ab initio. [b] e = experimental values which for the NgMX complexes have been derived from the centrifugal distortion constants using a diatomic approximation. a = ab initio values. [c] c = ab initio values for the complex. m = experimental values for the monomer. [d] Force constant k derived from ω(Ng−M) using a diatomic approximation. [e] Ab initio dissociation energies. c = corrected for basis set superposition error using the counterpoise correction. u = uncorrected for basis set superposition error. [f] Values for this complex from ref 1b or present work, except where stated otherwise. [g] Reference 35. [h] Reference 32. [i] Reference 36a. [j] Reference 36b. [k] Values for this complex from ref 37. Average values of D_e(Cu−Ng) are given. [l] Values for this complex from ref 1a or present work, except where stated otherwise. [m] Reference 38. [n] Reference 39. [o] Reference 40. [p] Values for this complex from ref 5 or present work, except where stated otherwise. [q] Values for this complex from ref 4, except where stated otherwise. [r] Present work, unless otherwise indicated. [s] Reference 3. [t] Reference 41; apparent typographical error corrected. [u] Reference 2. [v] Reference 42. [x] Reference 7. [y] Reference 44. [w] Reference 43; σ_g and σ_u stretching frequencies are given, respectively. Dissociation energies given are one-half the atomization energies.

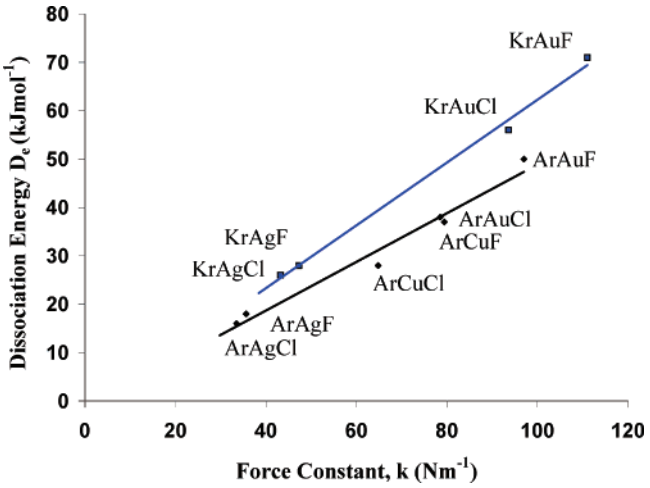

Figure 5. Plots of dissociation energy vs force constant for Ng−M bonds in NgMX complexes.

There is a strong correlation between the experimental force constants, k, and the ab initio dissociation energies, D_e. This correlation is shown in the graph in Figure 5. It is roughly consistent with a Morse potential, for which k is related to D_e by

$$k = 2D_e\beta^2 \qquad (5)$$

where β is the Morse potential constant. If β is constant for all molecules considered, then a graph of D_e vs k should be linear. Figure 5 shows this to be approximately the case. However, β is slightly different for the Ar- and Kr-containing complexes.

Nuclear Quadrupole Coupling. In the present work, nuclear quadrupole coupling has been observed for ^{197}Au, bromine (^{79}Br and ^{81}Br), and ^{83}Kr. The constants in each case have provided valuable information about the distribution of electron density at the given nucleus.

Table 8. ^{197}Au Nuclear Quadrupole Coupling Constants (MHz) in ArAuX and KrAuX Complexes and Related Species

molecule	eQq (^{197}Au) X = F	X = Cl	X = Br
AuX	−53.2[a]	9.6[b]	37.3[b]
ArAuX	−333.4[c]	−259.8[d]	−216.7[c]
KrAuX	−404.8[e]	−349.9[d]	
[XAuX]$^-$		−765[f]	−790[f]

[a] Reference 31. [b] Reference 42. [c] Reference 3. [d] Reference 2. [e] This work. [f] Reference 69.

The ^{197}Au coupling constant in KrAuF is radically different from that of AuF monomer.[31] The values are given in Table 8 in comparison with those of other AuX and NgAuX molecules measured to date, as well as those of XAuX$^-$ ions (valence isoelectronic with NgAuX). The changes in the ^{197}Au coupling constant on attachment of Ar to AuX are ∼250−280 MHz, which is roughly one-third of the change in going from AuX to XAuX$^-$. The changes on attachment of Kr are even larger, ∼350−360 MHz, which is 40−45% of the change when AuX forms XAuX$^-$. These changes are largely independent of halide. Complex formation clearly produces a significant reorganization of the electron distribution near the Au nucleus.

The changes in the Br coupling constants are less dramatic but valuable nonetheless. The coupling constants of AgBr, NgAgBr, and OCAgBr and the corresponding Cl coupling constants are compared in Table 9. In the absence of data on XAgX$^-$ ions, the carbonyl complexes are included as species where the ligand CO is strongly chemically bonded to Ag.[47] In

(47) Walker, N. R.; Gerry, M. C. L. *Inorg. Chem.* **2002**, *41*, 1236.

Table 9. Halogen Nuclear Quadrupole Coupling Constants (MHz) in AgBr, NgAgBr, and Related Species

parameter	AgX[a]	ArAgX	KrAgX	OCAgX
$eQq(^{79}Br)$	297.047[b]	278.888[b,c]	271.91[d]	223.902[b]
$eQq(^{35}Cl)$	−36.440[b]	−34.486[b,c]	−33.79[e]	−28.151[b]

[a] X = halogen. [b] Reference 47, Table 8, and references therein. [c] Reference 1a. [d] This work. [e] Reference 4.

Table 10. ^{83}Kr Nuclear Quadrupole Coupling Constants (MHz) for Various Linear Kr Complexes

molecule	$eQq(^{83}Kr)$	comments
Kr	0	
Kr−Ne	−0.52	ref 48
Kr−Ar	−0.85	ref 48
Kr−HCl	5.20	ref 49
KrAgF	105.10	this work
KrAuF	185.94	this work
KrD^+	549	ref 50
KrF_2	978	ref 51
Kr^+	915	ref 51; ab initio

these cases, the changes in the halogen coupling constant on addition of Ar to AgX are about one-quarter of those found on addition of CO to AgX; the corresponding changes on addition of Kr are near one-third. Again the fractional changes are large.

Given that the free Kr atom is spherically symmetric, so that $eQq(^{83}Kr) = 0$, the eQq values obtained for ^{83}KrAgF and ^{83}KrAuF (105.10 and 185.94 MHz, respectively) are quite remarkable. A dramatic distortion of the electron distribution at the Kr nucleus occurs on complex formation, with the greater distortion being for formation of KrAuF. This would appear to be consistent with the shorter Kr−Au bond (r(KrAu) < r(KrAg)) and the higher Kr−Au dissociation energy.

The measured ^{83}Kr coupling constants are compared to those of related molecules and ions in Table 10. The values range from very small and negative for very weakly bound KrNe and KrAr, through +5 MHz for KrHCl, which can be regarded as a "conventional" van der Waals complex, through the present complexes to the ions KrD^+ and Kr^+. Some implications of these results are treated in the following section.

Discussion

Table 7 shows that the structural properties of the two new complexes are consistent with those of the complexes previously reported. For example, for a given MX, the Kr−M bonds are all slightly (0.03−0.07 Å) longer than the corresponding Ar−M bonds. The variation with halogen atom of a given Kr−M bond length parallels that of the Ar−M bond length. Similarly, the force constants k(Kr−M) are all somewhat greater (by 8−16 N m^{-1}) than the corresponding constants k(Ar−M).

The ^{83}Kr nuclear quadrupole coupling constants in ^{83}KrAgF and ^{83}KrAuF have provided the first direct experimental information on the electron distribution on the noble gas atom in the complexes. The values are, not unexpectedly, considerably larger than those in weakly bound complexes such as ArKr or KrHCl but less than that of strongly bound KrD^+. They have prompted us to review the nature of the bonding in the complexes. Although the complexes might initially be considered as merely strongly bound van der Waals complexes, there is considerable evidence for weak chemical bonding, particularly for NgAuX. The deductions are made on the basis of both experimental and theoretical parameters. The former include the

Table 11. Comparison of Noble Gas−Noble Metal Bond Lengths (Å) in NgMX Complexes with Values Estimated from Standard Parameters

Standard Parameters

atom/ion	van der Waals radius (r_{vdW})	ionic radius (r_{ion})	covalent radius (r_{cov})
Ar	1.88[a]		0.94−0.95[b] (0.98)[c]
Kr	2.00[a]		1.09−1.11[b]
Xe	2.18[a]		1.30−1.31[b]
Cu^+/Cu(I)		0.60[d]	1.06[e]
Ag^+/Ag(I)		0.81[d]	1.28[e]
Au^+/Au(I)		0.77[d]	1.27[e]
Na^+		0.79[d]	

Bond Lengths (r(Ng−MX))

	experimental	$r_{vdW}(Ng) + r_{ion}(M^+)$	$r_{cov}(Ng) + r_{cov}(M(I))$
ArCuX	2.22−2.30	2.48	2.04
ArAgX	2.56−2.64	2.69	2.26
ArAuX	2.39−2.50	2.65	2.25
Ar−NaCl	2.89	2.67	
KrAgX	2.59−2.66	2.81	2.38
KrAuX	2.46−2.52	2.77	2.37

[a] Reference 52. [b] Reference 46. [c] Reference 53. [d] These are the values for coordination number 2. All are calculated from $r(M^+) = r(MF) - r(F^-)$. The values for Cu^+ and Ag^+ are from ref 54; those for Au^+ and Na^+ are newly calculated here. [e] Reference 55.

NgM bond lengths, the rigidity of the complexes, and the nuclear quadrupole coupling constants. The latter include ab initio bond lengths, NgM dissociation energies, molecular orbitals, and electron density distributions. Each of these aspects is considered below.

Ng−M Bond Lengths. The Ng−M bond lengths are presented in Table 11 in comparison with those calculated using various standard parameters. In one case, the comparison is with the sum of the noble gas van der Waals radius and the metal ionic radius. This is the perspective of van der Waals bonding. In all cases, the observed bond lengths are less than the sum given, with the smallest differences found for the AgX complexes; the largest (0.31 Å) is found for KrAuF. For a given MX, the differences are larger for the Kr−M bonds than for the Ar−M bonds.

The second comparison is with the sum of the noble gas and metal(I) *covalent* radii, also in Table 12. Now the differences are in the other direction, with the experimental bond lengths greater than the sum, by approximately the same amounts for the NgCuX and NgAuX. The differences are bigger for NgAgX. For a given MX, the differences are smaller for KrMX than for ArMX. So this evidence is ambivalent: neither comparison is conclusive.

To put this comparison in perspective, consider the corresponding difference for Ar−NaCl. Huheey et al.[54] give the ionic radius of six-coordinate Na^+ as 1.16 Å. If that of two-coordinate Na^+ is calculated by the same method as that for Cu^+, Ag^+, and Au^+ ($r_{ion}(Na^+) = r_e(NaF) - r(F^-)$), the result is $r(Na^+) =$

(48) Xu, Y.; Jäger, W.; Djauhari, J.; Gerry, M. C. L. *J. Chem. Phys.* **1995**, *103*, 2827.
(49) Campbell, E. J.; Buxton, L. W.; Keenan, M. R.; Flygare, W. H. *Phys. Rev. A* **1981**, *24*, 812.
(50) Warner, H. E.; Conner, W. T.; Woods, R. C. *J. Chem. Phys.* **1984**, *81*, 5413.
(51) Holloway, J. H.; Schrobilgen, G. J.; Bukshpan, S.; Hilbrants, W.; de Waard, H. *J. Chem. Phys.* **1977**, *66*, 2627.
(52) Pyykkö, P. *Chem. Rev.* **1997**, *97*, 597.
(53) Pyykkö, P. *Science* **2000**, *290*, 64.
(54) Huheey, J. E.; Keiter, E. A.; Keiter, R. L. *Inorganic Chemistry, Principles of Structure and Reactivity*, 4th ed.; Harper-Collins: New York, 1993.

Table 12. Comparison of MX Dipole Moments and Effective Atomic Charges, Induction Energies, and ab Initio Dissociation Energies of NgMX Complexes

	MX[a]		$-E_{ind}$[b]		D_e[b]		
complex	μ[a]	q_{eff}	μ/μ_{ind}[c]	q_{eff}/μ_{ind}[c]	uncor[d]	cor[d]	ref 32[e]
ArCuF	5.77[f]	0.69	8	22	47[g]	44	37
ArCuCl	5.2[h]	0.53	4	13	37[g]	33	28
ArAgF	6.22[f]	0.65	4	11	17	14	18
ArAgCl	6.08[i]	0.55	3	8	14[j]		16
ArAuF	3.4[h]	0.37	2	5	59[k]	55	50
ArAuCl	3.1[h]	0.29	1	3	47[l]	42	38
KrAgF	6.22[f]	0.65	5	16	32[m]	17	28
KrAgCl	6.08[i]	0.55	4	11	28[n]	15	26
KrAgBr	5.62[o]	0.49	3	8	25	17	
KrAuF	3.4[h]	0.37	3	6	86	58	71
KrAuCl	3.1[h]	0.29	1	4	71[l]	44	56
Ar−NaCl	9.00[p]	0.79	4	10	8[q]		
Ar−BeO	7.2[r]	0.84	26	84		45[r]	

[a] μ of the MX monomer in Debye; q_{eff} in fractions of an elementary charge. [b] $-E_{ind}$ and D_e in kJ mol^{-1}. [c] μ/μ_{ind} is the dipole-induced dipole value; q_{eff}/μ_{ind} is the charge-induced dipole term (see text). [d] Present work unless otherwise indicated: the corrected values account for basis set superposition errors (BSSE) using the counterpoise correction. [e] Reference 32; BSSE is accounted for. [f] Reference 33. [g] Reference 1b. [h] Estimated using eq 6 as described in the text. [i] Reference 59. [j] Reference 1a. [k] Reference 3. [l] Reference 2. [m] Reference 5. [n] Reference 4. [o] Reference 60. [p] References 61, 62. [q] Reference 7. [r] Reference 63.

0.79 Å, a much smaller value. This result is consistent with those of two-coordinate Cu^+, Ag^+, and Au^+ (Table 11). Consequently the sum of the Ar van der Waals radius and $r(Na^+)$ is 2.67 Å, considerably smaller than r(Ar−Na) in the complex (2.887 Å).[7]

Flexibility of the Complexes. The small centrifugal distortion constants are consistent with high rigidity for the complexes. They provide one of the most easily observed, and arguably most compelling, indications of unusually strong Ng−M bonding, with a probable unusual mechanism. They correlate well with the short Ng−M bond lengths. They also provide high Ng−M vibration frequencies (all of which are above 100 cm^{-1}) which agree with Ng−M values from the MP2 calculations. The NgM force constants range up to values which are approximately one-half that of KrF in KrF_2.[45]

Although the distortion constants refer only to the stretching vibrations, there is also an excellent indication that there is very little bending flexibility either. There are two perspectives on this: (i) Historically the reduction of the halogen coupling constant on complex formation (e.g., Br in AgBr) has been taken as a measure of the degree of a wide amplitude vibration. The equation used is

$$eQq = eQq_o\left\langle \frac{3\cos^2\beta - 1}{2} \right\rangle \qquad (6)$$

where eQq and eQq_o are the halogen coupling constants in the complex and monomer, respectively, and β is the bending angle. In KrAgBr, for example, this would produce $\beta \approx 13.7°$, indicating a significant degree of bending flexibility. However, if this were the only conclusion from the NQCCs, the *metal* coupling constants should show similar behavior. Clearly from Table 8 (and other sources[2]), this is not the case, so the NQCCs cannot be used in these cases as measures of bending flexibility. (ii) All the MX bond lengths in the complexes (e.g., r(AuCl)) are very close to those of the MX monomer, and experimentally no systematic difference has been found.[1−5] A van der Waals complex with flexible bending would be expected to show a significant decrease in the effective MX length; such a phenomenon even extends to flexible molecules which are unquestionably chemically bonded.[56] Given that van der Waals complexes often have substantially isotropic potentials between their constituents,[57] this provides further evidence that van der Waals interactions can provide at best only an incomplete picture of the bonding.

Again a contrast must be made with Ar−NaCl. The distortion constant of ArAgCl is ∼25 times smaller than that of Ar−NaCl. Since Ar−NaCl is very much a van der Waals complex,[7] this begs the question of what can be different between Na^+ and M^+ (Cu^+, Ag^+, Au^+) which can contribute to their bonding. Clearly this must be the availability for bonding of low-lying d-orbitals in the noble metals. The results of the ab initio calculations presented below show clearly that this is the case.

Ng−M Bond Energies. Although the ab initio dissociation energies are large, it is appropriate to compare them with purely electrostatic induction energies. Two approaches have been considered, namely dipole-induced dipole and charge-induced dipole, as representative of orders of magnitude to be expected.

Both approaches require knowledge of the dipole moments of the MX monomers. In most cases, experimental values could be obtained from the literature; for the others (CuCl, CuBr, AuF, AuCl, AuBr), dipole moments were estimated from ionic characters (i_c) calculated from halogen nuclear quadrupole coupling constants. The method used was that of Gordy and Cook, whereby i_c is converted to the dipole moment taking into account ionic polarizabilities. The equation was [ref 58, eqs 14.166 and 14.168]

$$eri_c = \mu\left(1 + \frac{\alpha_{M^+}}{[r^2 + (r_M/2)^2]^{3/2}} + \frac{\alpha_{X^-}}{[r^2 + (r_X/2)^2]^{3/2}}\right) \qquad (7)$$

Here e is the elementary charge, r is the MX bond length, α is the polarizability of the ion, and r_M, r_X are ionic radii. The values of i_c were taken from ref 42, except for AuF, whose value was estimated as $i_c = 0.5$ by extrapolation from AuBr and AuCl.[42] Ionic polarizabilities α from Gordy and Cook [ref 58, Tables 14 and 15] were used where possible; those of Cu^+ and Au^+ came from ref 8. All the dipole moments, both experimental and estimated, are in Table 12. From these, the ionic charges q_{eff} (elementary charge units) were estimated from the experimental bond lengths using

$$q_{eff} = 0.2082\frac{\mu(\mathrm{D})}{r(\text{Å})} \qquad (8)$$

These values are also in Table 12.

Now the induction energies could be estimated. The first method used was the dipole-induced dipole calculation, which superficially would seem reasonable, using the equation [ref 64, eq 10.16]:

(55) Pyykkö, P. *Chem. Rev.* **1988**, *88*, 579.
(56) Walker, K. A.; Evans, C. J.; Suh, S.-H. K.; Gerry, M. C. L.; Watson, J. K. G. *J. Mol. Spectrosc.* **2001**, *209*, 178.
(57) Frenking, G.; Koch, W.; Gauss, J.; Cremer, D. *J. Am. Chem. Soc.* **1988**, *110*, 8007.
(58) Gordy, W.; Cook, R. L. *Microwave Molecular Spectra. No. XVIII in Techniques of Chemistry*, 3rd ed.; Wiley: New York, 1984.
(59) Nair, K. P. R.; Hoeft, J. *J. Phys. B* **1984**, *17*, 735.
(60) Nair, K. P. R.; Hoeft, J. *Chem. Phys. Lett.* **1983**, *102*, 438.
(61) Hebert, A. J.; Lovas, F. J.; Melendres, C. J.; Hollowell, C. D.; Story, T. L.; Street, K. *J. Chem. Phys.* **1968**, *48*, 2824.

$$E_{ind} = -2\left(\frac{\alpha}{4\pi\epsilon_o}\right)\frac{\mu^2}{4\pi\epsilon_o r^6} \quad (9)$$

where $(\alpha/4\pi\epsilon_o)$ is the noble gas polarizability, μ is the MX dipole moment, and r is the distance from the Ng nucleus to the center of charge of the MX dipole ($= r_{NgM} + r_{MX}/2$). The results for several relevant MX monomers, including BeO and NaCl, are in Table 12. The values are ~20% of the ab initio dissociation energies.

However, eq 5 is valid really only at long distances, where contributions from both ends of the dipole are comparable. This is not the case for the NgMX complexes considered here. A more realistic approach might be to consider the effects of the individual charges at each end of the dipole. Because the Ng−M distance is very much shorter than the Ng−X distance, we will consider only the Ng−M contribution as an upper limit: the Ng−X contribution can be expected to reduce this value by about 10%. The equation used was [ref 64, eq 10.14]:

$$E_{ind} = -\left(\frac{\alpha}{4\pi\epsilon_o}\right)\frac{q_{eff}^2}{8\pi\epsilon_o r^4} \quad (10)$$

in which r is the Ng−M internuclear distance. The results of these calculations are also in Table 12. The contributions of the positive ion are roughly 2.5−4 times the values from the dipole-induced dipole calculations. Presumably the charge-induced dipole calculations are the more reliable. Even here, the long distance approximation is suspect, however, and the values for the positive ion may be low by as much as a factor of 1.5. Although these calculations would appear to support the view that the Ng−M binding energies are largely electrostatic, the variability of the ab initio values precludes any definite conclusion. In addition, there is a very significant *repulsive* electrostatic energy, even at r_e (ref 8, Tables 8 and 9), so the attractive energy should be substantially greater than the dissociation energy when the bonding is strictly electrostatic.

As further evidence, the results of the corresponding calculations for Ar−NaCl and Ar−BeO are also in Table 12. For the former, clearly a weakly bound van der Waals complex, the ion-induced dipole calculation accounts for *all* the ab initio dissociation energy, even in the (probably suspect) long-distance approximation. For the latter, which is strongly bound, and for which the binding energy is considered to be electrostatic in origin,[63] the positive ion-induced dipole calculation produces an induction energy which is roughly *double* an ab initio dissociation energy, again in the long-range approximation. These extremes are not reached for the present NgMX complexes, allowing for the possibility of other contributions to the Ng−MX dissociation energies.

^{83}Kr Nuclear Quadrupole Coupling Constants. If the bonding between the Ng atom and the MX molecule were purely electrostatic, this should be reflected in the nuclear quadrupole coupling constants and particularly those of ^{83}Kr. Sternheimer et al.[65] and, more recently, Fowler et al.[66] have each published several papers describing how an atom or ion with a spherical charge distribution is polarized by an external charge to produce a field gradient at its nucleus. In effect, the core electrons are subject to radial polarization via excitations np → p and nd → d. This polarization greatly magnifies the field gradient due to the external charge alone, by roughly 2 orders of magnitude. The field gradient is given by[66b]

$$V_{zz} = (1 + \gamma_\infty)E_{zz} + \epsilon_s E_z^2 \quad (11)$$

Here, E_z, E_{zz} are respectively the electric field and field gradient due to an external positive charge. γ_∞ is the Sternheimer antishielding constant, which is usually ~100.[49,67] ϵ_s is a constant characteristic of the noble gas. The nuclear quadrupole coupling constant is given by[49]

$$eQq = -eQV_{zz} \quad (12)$$

For both ^{83}KrAgF and ^{83}KrAuF, values of V_{zz} at the Kr nucleus were estimated using the geometries of Tables 6 and 4, respectively. The same fractional charges q_{eff} (Table 12) were used as in the estimates of the induction energy described above. Values for the field at the Kr nucleus due to an external positive charge (Ag^+ or Au^+) were calculated using

$$E_z = \frac{eq_{eff}}{4\pi\epsilon_o r^2} \quad (13)$$

where e is the elementary charge and r is the internuclear distance from the ion to Kr. The corresponding field gradient E_{zz} was obtained from

$$E_{zz} = \frac{dE_z}{dr} = -\frac{eq_{eff}}{2\pi\epsilon_o r^3} \quad (14)$$

The same expressions, with opposite signs, were used to calculate E_z (F^-) and E_{zz} (F^-). The resulting E_z and E_{zz} values used in eq 11 are the sums of the contributions from the corresponding cation and anion. Values of E_{zz} for each ion and their sums are given for the two complexes in Table 13.

The field gradient V_{zz} was then evaluated using eq 11. In the first term, which is dominant, the effect of electron polarization was estimated using $\gamma_\infty = 78$.[47] The contributions of this term to the eQq values were calculated using eq 12, with $Q(^{83}Kr) = 25.9$ fm^2.[68] The contributions for ^{83}KrAgF and ^{83}KrAuF are 43 and 29 MHz, respectively.

Table 13. ^{83}Kr Nuclear Quadrupole Coupling Constants Resulting from Polarization Due to External Charges

					eQq (MHz)	
complex	q_{eff}[a]	E_{zz}(M)	E_{zz}(F)	E_{zz}[b]	calcd[c]	exptl
KrAgF	0.65	−1.069	0.195	−0.874	43	105.10
KrAuF	0.37	−0.715	0.127	−0.588	29	185.94

[a] Fractional charge of the M^+ and F^- ions (Table 12). [b] E_{zz} is the sum of the field gradients at the Kr nucleus due to the M^+ and F^- ions (E_{zz}(M) and E_{zz}(F), respectively). Units are 10^{20} J C^{-1} m^{-2}. [c] Calculated using eqs 11 and 12 with $\gamma_\infty = 78$.[49]

(62) de Leeuw, F. H.; Van Wachem, R.; Dymanus, A. *J. Chem. Phys.* **1969**, *50*, 1393.
(63) Veldkamp, A.; Frenking, G. *Chem. Phys. Lett.* **1994**, *226*, 11.
(64) Berry, R. S.; Rice, S. A.; Ross, J. *The Structure of Matter: An Introduction to Quantum Mechanics*, 2nd ed.; Oxford: New York, 2002.
(65) Foley, H. M.; Sternheimer, R. M.; Tycko, D. *Phys. Rev.* **1954**, *93*, 734 and references therein.
(66) (a) Fowler, P. W.; Lazzeretti; P.; Steiner, E.; Zanasi, R. *Chem. Phys.* **1989**, *133*, 121. (b) Fowler, P. W. *Chem. Phys. Lett.* **1989**, *156*, 494.
(67) Keenan, M. R.; Buxton, L. W.; Campbell, E. J.; Balle, T. J.; Flygare, W. H. *J. Chem. Phys.* **1980**, *73*, 3523.
(68) Kellö, V.; Pyykkö, P.; Sadlej, A. J. *Chem. Phys. Lett.* **2001**, *346*, 155.

Table 14. Comparison of ^{79}Br and ^{83}Kr Nuclear Quadrupole Coupling Constants (eQq_o) and Field Gradients

	^{79}Br		^{83}Kr	
molecules	eQq_o/MHz	q_o[a]	eQq_o/MHz	%q_o[a]
DBr/DKr$^+$	530.648[b]	16.95	549.1	21.20
BrAuBr$^-$/KrAuF	202[c]	6.45	185.9	7.18
OCAgBr/KrAgF	223.9[d]	7.15	105.1	4.06
OCAuBr/KrAuF	285.1[e]	9.11	185.9	7.18

[a] *Relative* values ($\equiv eQq_o/eQ$ in MHz fm^{-2}) calculated using $eQ(^{79}\text{Br}) = 31.3$ fm^2 (ref 71) and $eQ(^{83}\text{Kr}) = 25.9$ fm^2 (ref 68). [b] Reference 72. [c] Reference 69. [d] Reference 47. [e] Reference 70.

The second term in eq 11 requires a value for ϵ_s. Fowler (ref 66b, Table 1) gives ~ -2.6 V^{-1} for Ar. The results in ref 67 (page 3528) give an estimate of ~ -11.1 V^{-1} for Xe. Since ϵ_s roughly follows the dipole−quadrupole hyperpolarizability,[66b] whose values are in ref 8, Table 5, we estimate ϵ_s for Kr ≈ -5 V^{-1}. The contributions of this term to eQq are thus $\sim$1−2 MHz and 0.10% of those of the first term (and possibly less than the uncertainty in γ_∞). Thus only the contributions of the first term are given in Table 13 and used in the discussion below.

The estimates of eQq (^{83}Kr) from eqs 11, 12, and 14 are compared with the experimental values in Table 13. It is immediately clear that the estimates account for only a fraction of the experimental values. This is especially so for KrAuF, where the calculated value is only one-sixth of the experimental one. Evidently polarization of the Kr atom by external charges is not the sole cause of the large values of eQq (^{83}Kr). Indeed it seems to be only a minor contributor, so that an alternative mechanism should be sought.

It is interesting to consider the present ^{83}Kr coupling constants in light of the value obtained for KrD$^+$ (549 MHz). Warner et al.[50] noted that the quadrupole moment of ^{83}Kr is very similar to those of ^{81}Br and ^{79}Br. From the eQq values for ^{83}KrD$^+$ and both D^{81}Br and D^{79}Br, they deduced that the field gradients at the Kr and Br nuclei were comparable. Since the two species are isoelectronic, they inferred that their electronic structures should be similar.

For our complexes, one valid comparison might be between ^{83}KrAuF and BrAuBr$^-$. For the latter, eQq (^{79}Br) has been calculated ab initio as 202 MHz.[69] (Although an experimental value would have been preferred, this value is reasonable: for other related complexes where calculated and observed values could be compared, the agreement was fairly good.[69]) Once again, the ^{83}Kr and ^{79}Br field gradients are comparable (see Table 14), prompting an inference that the electronic structures at the Kr and Br nuclei are similar in the two complexes.

Another possible comparison might be between ^{83}Kr in KrMF and ^{79}Br in OCMBr (M = Ag or Au). The ^{79}Br coupling constants in OCAgBr and OCAuBr are 223.9 MHz[47] and 285.1 MHz,[70] respectively. Given that the quadrupole moments of ^{83}Kr and ^{79}Br are 25.9 fm^2 and 31.3(3) fm,[2,71] respectively, the field gradients at ^{83}Kr are only slightly less than those at Br in the corresponding Ag- and Au-containing complexes; this is also shown in Table 14.

Electron Distributions from ab Initio Calculations. Besides the Ng−M and M−X bond lengths (Tables 4−7), Ng−M and M−X vibration frequencies (Table 7), and Ng−M bond dissociation energies (Table 7), the MP2 calculations also produced data on the electron distributions in the complexes. These took the form of Mulliken valence orbital populations for both KrAuF and KrAgBr, in which the orbital populations of atomic Kr, monomeric AuF or AgBr, and the complexes are compared. In addition, MOLDEN 3.4 plots of electron density were obtained for the 3σ and 1π valence molecular orbitals of both complexes.

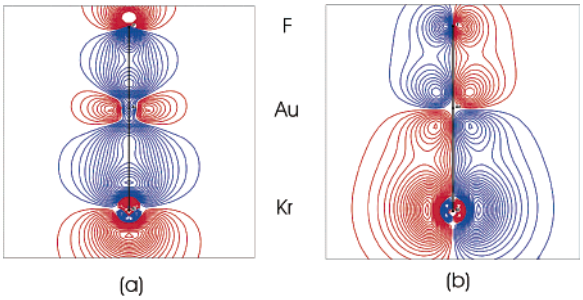

Figure 6. MOLDEN orbital contour diagrams for KrAuF: (a) 3σ and (b) 1π valence molecular orbitals. Each contour represents the enclosure of 1% of the electron density of each molecular orbital.

Table 15. Mulliken Valence Orbital Populations (n) for Kr, AuF, Kr−AuF, AgBr, and Kr−AgBr

orbital	Kr + AuF	Kr–AuF	orbital	Kr + AgBr	Kr–AgBr
Kr			Kr		
n_s	2.00	1.98	n_s	2.00	2.00
$n_{p\sigma}$	2.00	1.81	$n_{p\sigma}$	2.00	1.94
$n_{p\pi}$	4.00	3.98	$n_{p\pi}$	4.00	3.99
$n_{d\sigma}$	2.00	2.00	$n_{d\sigma}$	2.00	2.00
$n_{d\pi}$	4.00	4.00	$n_{d\pi}$	4.00	4.00
$n_{d\delta}$	4.00	4.00	$n_{d\delta}$	4.00	4.00
Au			Ag		
n_s	0.41	0.63	n_s	0.15	0.26
$n_{p\sigma}$	0.07	0.14	$n_{p\sigma}$	0.05	0.01
$n_{p\pi}$	0.12	0.08	$n_{p\pi}$	0.01	0.07
$n_{d\sigma}$	1.83	1.74	$n_{d\sigma}$	1.96	1.95
$n_{d\pi}$	4.00	4.00	$n_{d\pi}$	3.99	4.00
$n_{d\delta}$	4.00	4.00	$n_{d\delta}$	4.00	4.00
F			Br		
n_s	2.00	2.00	n_s	1.99	2.00
$n_{p\sigma}$	1.69	1.70	$n_{p\sigma}$	1.80	1.80
$n_{p\pi}$	3.84	3.84	$n_{p\pi}$	3.89	3.79
			$n_{d\sigma}$	2.00	2.00
			$n_{d\pi}$	4.00	4.00
			$n_{d\delta}$	4.00	4.00

The Mulliken populations are in Table 15. For both complexes, the most striking results are the changes in Kr orbital populations on complex formation. For KrAuF, there is apparently a σ-donation of 0.21 electron from Kr to AuF and a rather smaller π-donation. The former is apparently taken up mostly by the 6s and 6p$_\sigma$ orbitals on Au, with a slight drop in the 5d$_\sigma$ population. A very comparable result was found for KrAuCl.[2] (It is interesting that these values are about one-half the values for the donation from Xe to Au^{2+} in AuXe$_4^{2+}$,[10] so our results are consistent with these.) The corresponding values for ArAuF and ArAuCl are 0.12−0.14 electron.[2,3] The calculated donation to Ag is significantly less, being about 0.06−0.07 electron for all KrAgX complexes.

The orbitals depicted in the MOLDEN plots of Figures 6 and 7 are all doubly occupied for the complexes in their ground electronic states. They all suggest significant sharing of electron density between 4p orbitals on Kr and 4d and 5d orbitals on

(69) Bowmaker, G. A.; Boyd, P. D. W.; Sorrenson, R. J. *J. Chem. Soc., Faraday Trans. 2* **1985**, *81*, 1627.
(70) Evans, C. J.; Reynard, L. M.; Gerry, M. C. L. *Inorg. Chem.* **2001**, *40*, 6123.
(71) Pyykkö, P. *Mol. Phys.* **2001**, *99*, 1617.
(72) De Lucia, F. C.; Helminger, P.; Gordy, W. *Phys. Rev. A* **1971**, *3*, 1849.

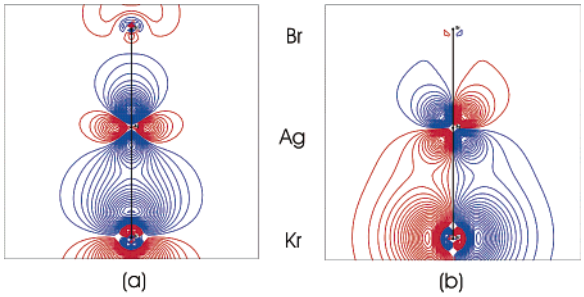

Figure 7. MOLDEN orbital contour diagrams of KrAgBr: (a) 3σ and (b) 1π valence molecular orbitals. Each contour represents the enclosure of 1% of the electron density of each molecular orbital.

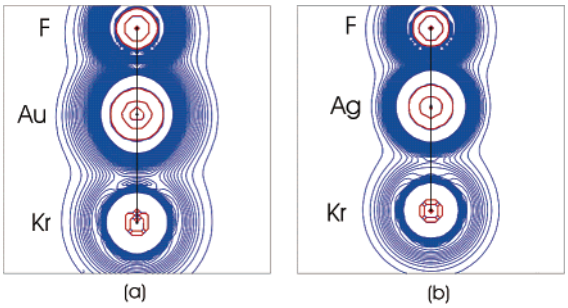

Figure 8. Contour plots of the Laplacian concentrations of the electron density, $-\nabla^2\rho(r)$, of (a) KrAuF and (b) KrAgF.

Ag and Au, respectively. The σ-sharing is greater than the corresponding π-sharing. The sharing appears to be especially strong for KrAuF and comparable to that of KrAuCl.[2] That of KrAgBr is comparable to those of KrAgCl[4] and KrAgF.[5]

Another ab initio criterion for chemical bonding is provided by the contours of the Laplacian distribution of the electron density, $\nabla^2\rho(r)$. This is an approach promoted by Frenking and co-workers in discussing the nature of the bonding in Ng−BeO complexes.[57,63] Basically distortion of the contours of the Laplacian concentration, $-\nabla^2\rho(r)$, for the Ng atoms was deemed to be an indication of the degree of covalency of the Ng−Be bond. For Ng−BeO, the distortion increased in the order Ar < Kr < Xe.[63] A distinct lobe for Xe in Xe−BeO was taken to indicate an onset of covalent bonding. Results of equivalent presentations for KrAuF and KrAgF are presented in Figure 8. Although there is some distortion for Kr, it is slight, so by this criterion the bonding is considered largely electrostatic.

Conclusions

The microwave rotational spectra of two new noble gas−noble metal halide (NgMX) complexes (KrAuF and KrAgBr) have been measured, and their rotational constants, centrifugal distortion constants, and nuclear quadrupole coupling constants have been precisely evaluated. In addition, transitions of a new isotopomer of KrAgF, namely $^{83}Kr^{107}Ag^{19}F$, have been measured, and its constants determined. Geometries of all three complexes have been evaluated.

The very first Ng nuclear quadrupole coupling constants for NgMX complexes have been measured. Very large values of eQq (^{83}Kr) have been found for KrAgF (105.10 MHz) and KrAuF (185.94 MHz). Since these values for uncomplexed Kr are zero, they represent a significant distortion of the electron cloud on complex formation. These results have triggered a major reassessment of the nature of the Ng−M bonding in all complexes observed to date.

The dilemma is whether the Ng−M bonds arise through purely electrostatic van der Waals interactions or whether some form of chemical bonding, particularly covalent bonding, is present. Several approaches have been considered. Charge-induced dipole induction energies appear to reproduce significant portions of the ab initio dissociation energies, but the fractions are much smaller than those of other nominally van der Waals complexes. Laplacians of the electron density suggest little buildup of electron density between the nuclei. On the other hand, Ng−M bond lengths are significantly shorter than the sums of noble gas van der Waals radii and M^+ ionic radii. For NgCuX and NgAuX complexes, the Ng−M bond lengths are closer to the sums of Ng and M covalent radii. The NgM bonds are rigid and apparently strongly anisotropic, in contrast to the usual situation for van der Waals bonds. Differences in the properties of NgMX and Ar−NaCl would seem to result only from participation of low lying valence d orbitals on the noble metals in the bonding.

The nuclear quadrupole coupling constants indicate a significant rearrangement of electron density on complex formation. Although this could conceivably be of electrostatic origin, an analysis of the ^{83}Kr coupling constants does not confirm this. The field gradients at Kr are very close to those at Br in isoelectronic complexes. The ab initio calculations indicate weak electron donation from Ng to M (~0.2 electrons in KrAuF), and MOLDEN plots of occupied valence molecular orbitals are consistent with Ng−M electron density sharing.

In the end, although there is no conclusive proof of NgM chemical bonding, there is ample evidence that it is occurring. While the case is weak for Ag, it is stronger for Cu and compelling for Au (and supported by the data on the $NgAu^+$ ions[8]). A definitive conclusion is hampered by the absence of a clear definition of a chemical bond and of a clear criterion for such bonding, particularly an experimental one. A recent exchange in the literature illustrates the dilemma.[73,74] For our purpose, we will consider chemical bonding to be occurring between two atoms if electron density on one atom when they are not bonded can have a significant probability of being in the sphere of influence (orbitals?) of the other atom when they are bonded. Since none of the experimental parameters can be fully accounted for by assuming that the noble gas and metal halides are simply nestled against each other and several ab initio results conform to our definition, we conclude that NgM chemical bonding is occurring, albeit weakly, in the noble gas−noble metal halide complexes. The effect should be greater for XeMX complexes; spectra of several have now been observed, and the analysis is underway.

Acknowledgment. This research has been supported by the Natural Sciences and Engineering Research Council of Canada and by the Petroleum Research Fund, administered by the American Chemical Society.

Supporting Information Available: Measured transition frequencies. This material is available free of charge via the Internet at http://pubs.acs.org.

JA0304300

(73) (a) Frenking, G. *Angew. Chem. Int. Ed.* **2003**, *42*, 143. (b) Frenking, G. *Angew. Chem. Int. Ed.* **2003**, *42*, 3335.
(74) Gillespie, R. J.; Popelier, P. L. A. *Angew. Chem. Int. Ed.* **2003**, *42*, 3331.